

Effect of Observation by Angle Only Navigation to Plan Non-Cooperative Approach for ADR

By Masayuki Ikeuchi¹⁾

¹⁾ Safety and Mission Assurance Department, JAXA, Sagamihara, Japan

(Received June 21st, 2017)

The objective of this paper is to study the effect of observation by Angle Only Navigation to plan non-cooperative Active Debris Removal approach for debris mitigation, and to have a concept of criteria for safe operation and mission assurance.

Key Words: Observation, AON (Angle Only Navigation), Non-Cooperative approach, ADR (Active Debris Removal)

Nomenclature

a	: semi measure axis
ave	: average
BL	: baseline
C	: non-linear observation matrix
CVL	: curvilinear
D	: representative diameter of target
DCR	: dual co-elliptic rendezvous
h	: relative height
e	: eccentricity
i	: inclination
L	: relative length
$LVLH$: local vertical local horizontal
$p(\Delta v)$: length or vector of BL by Δv
r	: radius
R	: range
rms	: root mean square
RM	: ranging model
SOR	: stable orbit rendezvous
v	: velocity
x	: state vector
δ	: error
φ	: elevation angle
η	: azimuth angle
ω	: augment of perigee, or target angular size
Ω	: ascending node

Subscripts

0-3	: number of RM
C	: chaser
T	: target

1. Introduction

It is necessary and important to have any visual reference information or criteria of ADR approach for safety and mission assurance, estimating its ranging accuracy and confirming observability in case of applying AON, and those

requirements or conditions for orbital planning about non-cooperative ADR approach are studied, because the ranging accuracy, derived from observed elevation and azimuth angles of a target by a chaser, seems to depend on the position and velocity of each planned relative orbit. Fig. 1. shows a typical relative orbit as the back ground,¹⁾⁻⁴⁾ of this study. This paper discusses (1) the condition of AON which can provide observability, (2) some approximations of ranging formulation, (3) some necessary augmented data from other sensors such as GPS, and (4) the amount of ΔV to keep the observability of relative navigation for ADR approach.

As in general the requirements for ADR approach orbit, the orbital safety against the thruster failure shall require such a planning that avoids any collision between the chaser and Target, and this paper discusses the relationship between the ranging accuracy and observability mentioned above and orbital safety by using some criteria.

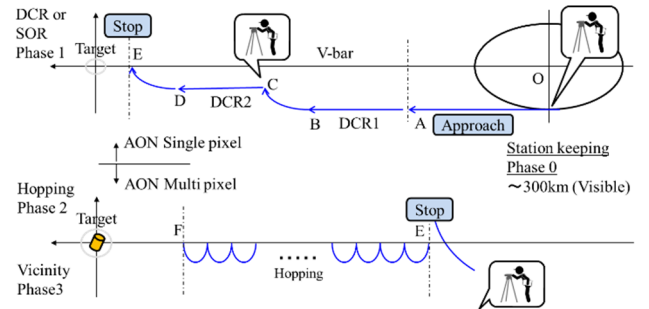


Fig. 1. Typical relative approach orbit. Chaser starts from Station keeping (Phase 0), goes through DCR or SOR (Phase 1), Hopping (Phase 2), V-bar approach, Fly Around, and Final Approach to Target (Phase 3).

2. Observation

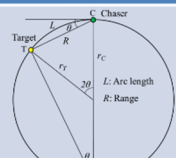
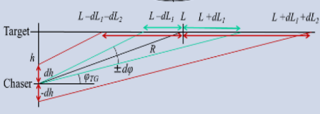
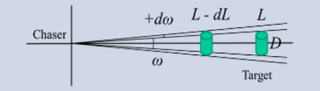
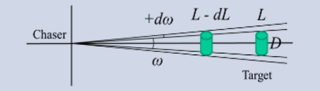
2.1. Coordinates

Fig. 2. shows the coordinates to define measurements.

It is noted that there are two definitions here expressing the Target elevation angle φ . In this paper, the arc length from Chaser to Target $y_{T.HILL} = L_T$ is used as range.

The difference between RM1 and RM2 is if there is any orbit control or not. RM1 based on Fig. 3 expects only static ranging without control. However, RM2 includes any control for ranging. RM3, based on multi pixel of Target object, is not a kind of AON. However, RM3 is used to confirm switching from single pixel navigation to multi pixel navigation.

Table 1. Ranging Models.

RM	Target	L/δ	Ranging Scheme	Ranging Model
RM0 (Phase 0~1)	Single Pixel	L/δ_0	- Curve linear. - Observing Target light in Single Pixel	
RM1 (Phase 0~1)	Single Pixel	L/δ_1	- Estimated BL - Target OD data or Chaser GPS	
RM2 (Phase 0~2)	Single Pixel	L/δ_2	- Estimated BL - ΔV calibrated	
RM3 (Phase 2~3)	Multi Pixel	L/δ_3	- Target object by Multi Pixel	

The objective of Table 1. is to confirm such area that gives high ranging accuracy by using non-dimensional criteria L/δ . If this is possible, it is expected to plan a relative approach orbit generally, and to make it easier to have initial and final conditions of each area.

3. Condition of AON Providing Enough Accuracy

3.1. Static Prediction of Ranging Accuracy

Fig. 5. is an example of integrated navigation chart for ranging with respect to Table 1., with a set of some defined parameter. Here, whole area related to a relative approach, is decomposed first by using Table 1. with respect to Phase 0 ~ 3 in Fig. 1., and composed again as integrated Area connected by squares of blue line, where all ranging models can be satisfied in the basis of $L/\delta_N > 30$. Phase “n” in Fig. 5. are related to relative orbit in Fig. 1. Every interface between each Area is shown as blue arrows. The lower interface of height is drawn tentatively as 3km between Area 0 and Area 1, hoping less Δv consumption, but this height is not so sensitive in Area 0. There is no need to confirm the observability in Area 0 by using linear control theory. It is also recognized that SOR orbit has poor ranging accuracy near v-bar above Area 1.

3.2. Phase 0 Circle Ranging

RM0 is simulated to validate the feasibility of this application by L/δ_0 . After Fig. 5. is derived, it is easier than before to find a reasonable initial condition of Phase 0. Fig. 6. is an example of relative orbit of Phase 0 based on the LVLH coordinate defined in Fig. 2. Chaser (SAT1) is planned as relative station keeping, but it is gradually approaching Target (SAT3). The objective is to estimate this relative orbit of Target by the orbital parameters of Chaser as known and AON without relative propagation. The major results of RM0 are shown in Table 2. “t” is when $\varphi_{T \max}$ is observed, and $\varphi_{T \min}$ is measured just before each observation of $\varphi_{T \max}$. L/δ and h/δ are in high accuracy, except h/δ at $t = 170477$ sec (~46hour). This may be affected by the integration or its interval.

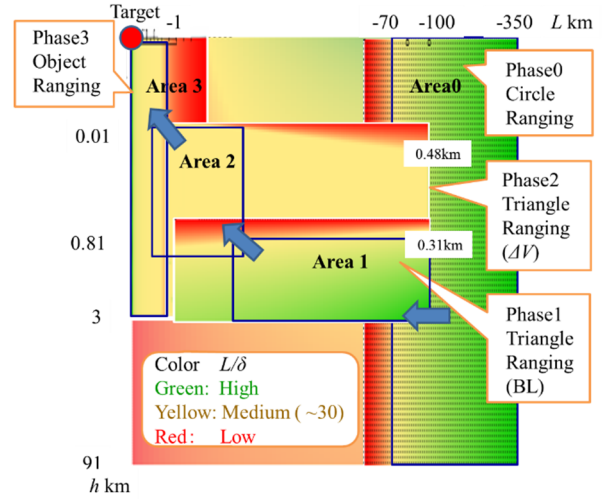


Fig. 5. Integrated Navigation Chart for Ranging (static). Area “n” is related to L/δ_n , and blue square in each Area

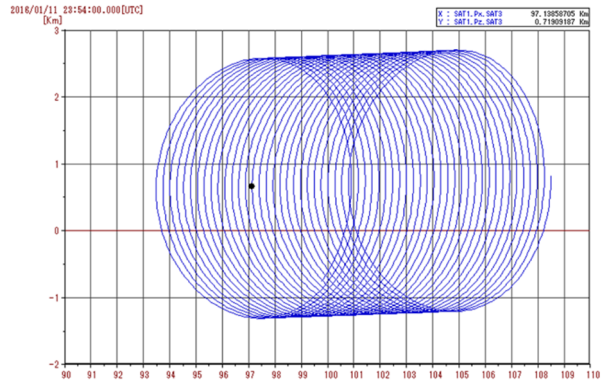


Fig. 6. Phase 0 Simulation to confirm L/δ_0 . Target: $a = 7078.136$ km, $e = 0.00104637$, $i = 98.192$ deg, $\Omega = 109.947$, $\omega = 90.000$ deg, $M = 0.000$ deg, Chaser relative initial condition: $(x_c, y_c, z_c) = (0, -108511.82, -0.02)$ [m], $(v_{x_c}, v_{y_c}, v_{z_c}) = (-2.167, -0.011, 0)$ [m/s] in CVL by special perturbation for two days, with J_{12} and gravity of Sun and moon.

Table 2. Simulation results of L/δ_0

t	s	4460	170477
$\varphi_{T \max}$	deg	1.48	1.52
$\varphi_{T \min}$	deg	-0.66	-0.77
L/δ		157.2	129.7
h/δ		113.4	32.4

Also, the approach speed is estimated in case of Table 2., as 0.052m/s, whereas the simulation result is 0.044m/s.

Another simulation of $L = 110 \sim 125$ km is tried, which is a farther case than Table 2. Fig. 5. suggests better L/δ will be acquired, and the results are so agreeable as $L/\delta = 311.2, 154.7$ and $h/\delta = 51.6, 40.7$ respectively. Here, estimated approaching velocity is 0.037m/s, whereas the simulated speed is 0.035m/s. For $\delta a = -0.0207$ km, the estimated results at each moment is $\delta a = -0.0177, -0.0200$ km. However, in the case of Table 2., Chaser is in eclipse when $\varphi_{T \max}$ is observed, and so it will be necessary to interpolate the history of elevation angle by using only sunlit data to estimate $\varphi_{TG \max}$ using proper model.^{4), 5)}

3.3. Phase 1 Triangle Ranging with Baseline (BL)

Fig. 7. shows an example of DCR in LVLH coordinate, and the curve includes both absolute orbit (slope) and relative orbit (sinusoidal). Because RM1 depends on CVL coordinate, the elevation shall be transformed from φ_T in LVLH to φ_{TG} in CVL frame as follows;

$$\begin{aligned} \varphi_{TG} &= \text{atan} \{ (2r_T \theta (\varphi_T + \theta) / (2rc \theta)) \} \\ &\sim (r_T / r_C) (\varphi_T + \theta) \\ &\sim \varphi_T + \theta \end{aligned} \quad (7)$$

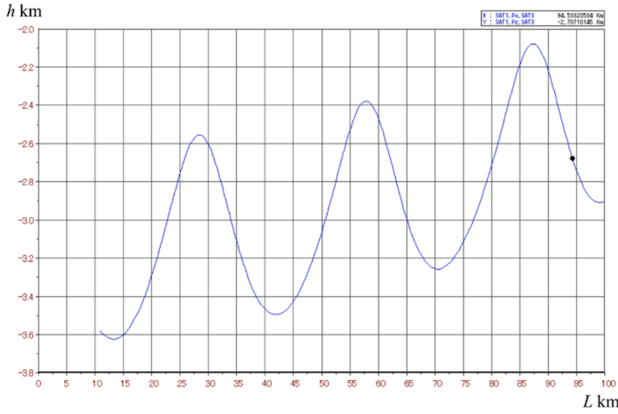


Fig. 7. Phase 1 Simulation to confirm L/δ_l . Target: $a = 7078.136\text{km}$, $e = 0.00104637$, $i = 98.192\text{deg}$, $\Omega = 109.947$, $\omega = 90.000\text{deg}$, $M = 0.000\text{deg}$, Chaser relative initial condition: $(x_C, y_C, z_C) = (-3608.59, -99940.46, 0.02)$ [m], $(v_{x_C}, v_{y_C}, v_{z_C}) = (0.0, 6.0, 0)$ [m/s] in CVL by special perturbation for five hours, with J_{12} and gravity of Sun and moon.

Table 3. shows the results of $L/\delta_l = 666.4$ in case of Fig. 7., where true model means the simulation using $\varphi_T + \theta$ in Eq. (7), and error model includes such an allowable set of errors that provides $L/\delta > 30$. Especially the initial error of L is assumed $L/\delta = 100$ as the result of Table 2, and the allowable error of h_T in LVLH frame is assumed as $0.071 = \sqrt{2} * 50\text{m}$, which means that RM1 is observable in theory,¹⁾ but may not be practically observable,⁶⁾ as this model without these support data.

Table 3. Simulation results of L/δ_l

Parameter	Source	True Model	Error Model	Input Error
φ_T deg	Obs by Cam	-2.70	-2.69	0.010
r_C km	Obs by GPS	7070.8	7070.83	0.030
L km	Sim	68.401	69.085	0.684
h_T (LVLH) km		-3.221	-3.150	0.071
θ deg		0.277	0.280	-
θ rad		0.005	0.005	-
r_T km		7067.910	7068.018	-
h_T (Hill) km		-2.890	-2.812	-
L km	Est in Hill	68.298	66.822	-
L/δ		666.4	30.5	-
L km	Est in LVLH	61.925	60.713	-
L/δ		10.6	8.3	-

If the amplitude of sinusoidal part ($\sim 1\text{km}$) in Fig. 7. is measured accurately by only GPS of Chaser, it can be used as a BL as shown in Fig. 3. to make RM1 accurate and observable in a special condition like DCR, where the apsis of both Chaser and Target are closely in a line.

3.4. Phase 2 Triangle Ranging with Δv

In Fig. 3. both RM1 and RM2 are applicable in similar area.

It is studied that an orbital maneuver can provide observability.^{7), 8)} Fig. 8. shows two examples of maneuver, and $p(\Delta v)$ called as ‘‘Proving’’ to provide observability. ‘‘ $p(\Delta v)$ ’’ is a kind of BL, and it is the difference of these two models that RM2 only gives observability with maneuvering.

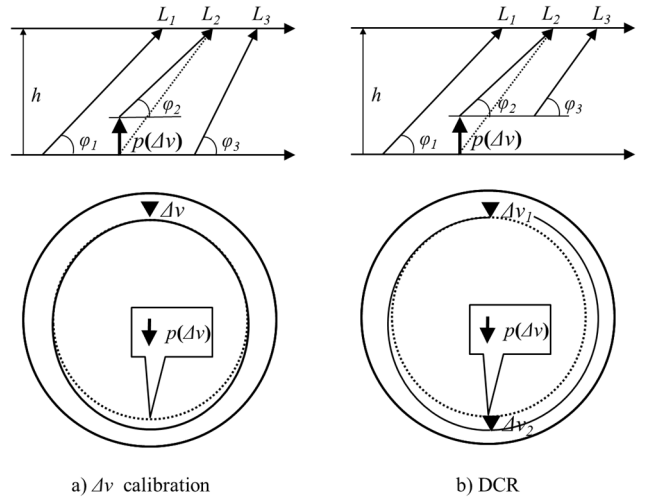


Fig. 8. Examples of observable situation with Δv . a) and b) give observability with maneuver.

3.4.1. Δv Calibration

As an example, perigee or apogee up maneuver can be a Probing, that is, $p(\Delta v)$ for navigation. Table 4. shows a simple relationship between control and navigation. In this case, δh is 7m, if $h > 280\text{m}$, but δh will be $< 7\text{m}$, if $h < 280\text{m}$.

Table 4. Orbital control, Probing, and navigation error

Orbital control		$P(\Delta v)$	Nav. Error	Note
Δt s	Δv m/s	Δh m	$\delta \Delta h$ (δP) m	
10	0.075	280	7	Δv calib.
5	0.0375	140	3.5	
1	0.0075	28	0.7	Δv calib.
0.5	0.00375	14	0.35	GPS accuracy
0.1	0.00075	2.8	0.07	
0.05	0.001875	1.4	0.035	

Condition: GPS data measured 4 times, accuracy $14\text{m}/\sqrt{4}$ (samples) = 7m for perigee/apogee up maneuver. Chaser mass: 400kg, Thruster: 3N, $\Delta h/\delta \Delta h = 40$ (=280/7).

By this Δv calibration shown Fig. 9. a), better $\delta p(\Delta v)$ is expected as following condition;

- 1) $\delta\Delta v_{GPS}$ and δv_{GPS} are applied if $h > h_{CP}$ (Calibration Point)
- 2) $\delta\Delta v_{THR}$ and δh_{THR} are applied, if $h < h_{CP}$,
where $\delta h_{THR} = \delta h_{GPS} * \delta\Delta v_{THR} / \delta\Delta v_{GPS}$

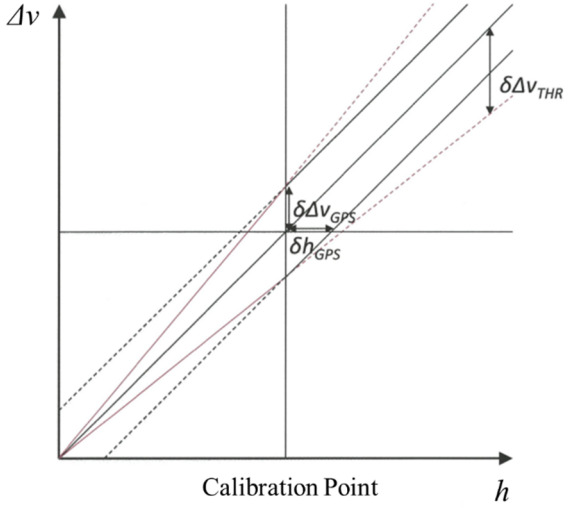


Fig. 9. Δv calibration. After a height transfer (perigee/apogee up or down) of h_{GPS} measured as $p(\Delta v)$ by Δv_{GPS} , $\delta\Delta v_{GPS}$ and δh_{GPS} are estimated at calibration point and $\delta\Delta v_{THR}$ is predicted.

3.4.2. Condition of AON Providing Observability

Let's discuss DCR in Fig. 9. b) simply as follows;

$$\alpha_1 = \tan \varphi_n = \frac{h_0}{L_n + v_n t} \quad (8)$$

$$\alpha'_n = \tan \varphi_n = \frac{h_0 - p(\Delta v)}{L_n + v_n t} \quad (9)$$

for $n = 2$ and 3 , that is, second and third observation.

By using (8) and (9), following matrix is composed to understand the situation, when RM2 is applied. Here it is so approximated that v_n are constant simply.

$$\begin{bmatrix} \alpha_1 & \alpha_1 t & -1 \\ \alpha'_2 & 2\alpha'_2 t & -1 \\ \alpha'_3 & 3\alpha'_3 t & -1 \end{bmatrix} \begin{bmatrix} L_0 \\ v_0 \\ h_0 \end{bmatrix} = \begin{bmatrix} 0 \\ -p(\Delta v) \\ -p(\Delta v) \end{bmatrix} \quad (10)$$

(10) is to be written as (11).

$$\mathbf{C}(t)\mathbf{x}_0 = \mathbf{p}(\Delta v) \quad (11)$$

\mathbf{x}_0 will be solved by (12), and $\delta\mathbf{x}_0$ is derived as (13) and (14), if $\mathbf{p}(\Delta v)$ is not 0, which means Δv performed.

$$\mathbf{x}_0 = \mathbf{C}(t)^{-1}\mathbf{p}(\Delta v) \quad (12)$$

$$\delta\mathbf{x}_0 = \mathbf{C}(t)^{-1} \left\{ \delta\mathbf{p} - \left(\frac{\partial\mathbf{C}(t)}{\partial\varphi} d\varphi + \frac{\partial\mathbf{C}(t)}{\partial t} dt \right) \mathbf{x}_0 \right\} \quad (13)$$

where

$$\frac{\partial\mathbf{C}(t)}{\partial\varphi} d\varphi + \frac{\partial\mathbf{C}(t)}{\partial t} dt \quad (14)$$

$$= \begin{bmatrix} \frac{1}{\cos^2\varphi_1} & \frac{t}{\cos^2\varphi_1} & 0 \\ \frac{1}{\cos^2\varphi_2} & \frac{2t}{\cos^2\varphi_1} & 0 \\ \frac{1}{\cos^2\varphi_3} & \frac{3t}{\cos^2\varphi_1} & 0 \end{bmatrix} d\varphi + \begin{bmatrix} 0 & \tan\varphi_1 & 0 \\ 0 & 2\tan\varphi_2 & 0 \\ 0 & 3\tan\varphi_3 & 0 \end{bmatrix} dt$$

It is interesting that (11) seems to be linear control model at a glance, but it is non-linear, and it is visualized that some interaction between control and navigation is expected.

In case of (8) and (9), $\mathbf{p}(\Delta v)$ is vertical, but the same equation as (11) can be shown with similar components in its matrix. As approaching to Target, Δv decreases so small that (12) could fail finally, and RM2 also has its approaching limit, and it will be succeeded by RM3.

3.5. Phase 3 Object Ranging

Phase 3 is a terminal condition of AON to switch object ranging RM3. During continuous thrusting, longer than one second, the condition to estimate $\delta p(\Delta v)$ expected as 1) above Fig. 10. However, impulsive thrusting, shorter than one second, further Δv calibration will be necessary for the final approach to estimate $\delta p(\Delta v)$ expected as 2) above Fig. 10..

The objective is to find where the later calibration will be done for impulsive thrusting.

When $\Delta t = 1s$, $P(\Delta v) = 28m$ in Table 4, and if along track movement of Chaser is twice $P(\Delta v)$, assuming relative station keeping, and if $L/\delta_2 = 30$, then $L = 28 * 2 * 30 = 1680m$.

Fig. 10. depicts what kind of the image of Target by camera is at near range, and it is recognized that L/δ_2 is much higher than L/δ_3 . Thus, the final Δv calibration point will be a relative station keeping orbit. To have a planned intersection of L/δ_2 and L/δ_3 like Fig. 10, hopping approach with periodical Δv will be suitable to switch from high L/δ_2 to L/δ_3 , waited for increasing enough value, as an example, 80 by $FOV = 10deg$ as shown Fig. 10. As written in Table 1, L/δ_3 is for multi pixel ranging, and it is interesting that L/δ_3 is nearly proportional to the number of pixels, which means 80 pixels seen for a representative length of Target.

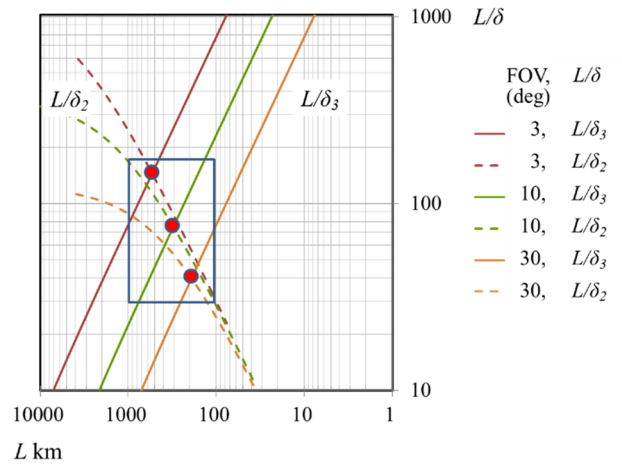


Fig. 10. Switching from L/δ_2 to L/δ_3 . D of Target is 4m, FOV's are examples, and hopping approach is assumed here.

3.6. Amount of Δv to keep Observability of AON

Through Phase 0 to Phase 3, the total amount of Δv is due to a) transferring height h to v -bar, b) total length of hopping, c) station keeping, and d) other corrections.

3.7. Navigation Chart

Fig. 5. and Table 5. summarize a proposed Navigation chart (static and dynamic), which give navigation maps visualized based on the variation of parameter related to sensors and operation, by applying quality engineering. Fig. 5. will be updated on-line while mission operation, and Table 5. will contribute as a guideline for relative orbit planning. These results are cooperative with safe approach design, and no contradiction is confirmed so far.

Phase 0 is in a preferable condition for optical navigation (RM0). The approach limit of RM0, pure AON depends on 1 sample in Table 5. The limit can be nearer Target if samples are increased. The approach limit of RM1 itself is estimated as 8~16km, but can approach up to 3km or nearer, if supported by some data or RM2, which will contribute in a range of 100m~8km in Phase 2. RM2 seems sensitive. To keep robustness of RM2, the operational range will be suitably short. In Phase 3, RM3 is so designed to take over navigation from AON.

Table 5. Navigation chart (dynamic).

RM	Target	L/δ	Simulation condition	Approach Limit	Observability	Ranging Accuracy ($L/\delta > 30$)
RM0 (Phase 0~1)	Single Pixel	L/δ_0 Circle	$d\theta = 0.01 \text{ deg.}$ $h \sim 0 \text{ km.}$ $dh = N/A$	$ L > 75 \text{ km}$ due to $d\theta$	- Observable - Higher L/δ_0 by longer L . - dh is not sensitive.	
RM1 (Phase 0~1)	Single Pixel	L/δ_1 Base line	$d\varphi = 0.01 \text{ deg.}$ $dh = 27.55 \text{ m}$	$ L > 8 \sim 16 \text{ km}$ $ h < 1.2 \text{ km}$ due to dh	- Observable with augmented data, e.g. OD and GPS.	
RM2 (Phase 0~2)		L/δ_2 ΔV calib.	$d\varphi = 0.01 \text{ deg.}$ $dh = 0.5 \text{ m}$	$ L > 100 \text{ m.}$ $ h > 30 \text{ m}$ due to dh	- Observable with ΔV - Approach limit improved by ΔV calib.	
RM3 (Phase 2~3)	Multi Pixel	L/δ_3 Object	$d\omega = 0.01 \text{ deg.}$ $dh = N/A$	$ L < 600 \text{ m}$ due to $d\omega$	- Observable	

Approach Limit Estimated with criteria $L/\delta > 30$

4. Conclusion

In this paper, the effect of observation by AON in Low Earth Orbit to plan non-cooperative approach has studied, and the following items are summarized;

- Navigation chart proposed.
 - where
- Visual map of ranging accuracy for optical navigation.
- Unified and non-dimensional simple criterion as L/δ for ranging accuracy, expected to be useful also for other optical navigation.
- Observability studied as follows;
 - difference of observability confirmed between true model with no relative propagation and algorithm using Hill equation as a relative propagation model.
 - Observability of true model checked by simulation, and compared with references. ^{1), 6)}
 - Suitable area or orbit phase visualized for keeping accuracy ranging.
 - Other suitable condition provided by sensor and operation.

References

- 1) Yamamoto. T., Murakami N., Nakajima Y., Yamanaka K.: *Navigation and Trajectory Design for Japanese Active Debris Removal Mission*, 24th International Symposium on Space Flight Dynamics, 2014, S9-5.
- 2) Woffinden, D. C. and Geller D. K.: *Navigating the Road to Autonomous Orbital Rendezvous*, Journal of Spacecraft and Rockets, Vol. 44, No. 4, 2007, pp. 898-909.
- 3) Geller D. K. and Klein I.: *Angles-Only Navigation State Observability During Orbital Proximity Operations*, Journal of Guidance, Control, and Dynamics, Vol. 37, No. 6, 2014, pp. 1976-1983.
- 4) G. Gaias, S. D'Amico, and J. S. Ardaens.: *Angles-Only Navigation to a Noncooperative Satellite Using Relative Orbital Elements*, Journal of Guidance, Control, and Dynamics, Vol. 37, No. 2, 2014, pp. 439-451.
- 5) Yamanaka, K., Ankersen, F.: *New State Transfer Matrix for Relative Motion on an Arbitrary elliptical orbit*, Journal of Guidance, Control, and Dynamics, Vol. 25, No. 1, 2002 pp. 60-66.
- 6) Grzymisch, J., Fichter, W.: *Observability Criteria and Unobservable Maneuvers for In-Orbit Bearings-Only Navigation*, Journal of Guidance, Control, and Dynamics, Vol. 37, No. 4, 2014, pp. 1250-1259.
- 7) Ikeuchi, M., Kawamoto. S.: *Small Space Debris Sweeper with Probing*, 18th IFAC, September 2010.
- 8) Ikeuchi, M., Tanabe T.: *New Concept for Autonomous Rendezvous Approach Navigation and Guidance System Using Only Target Image Information*, 11th IFAC, July 1989.